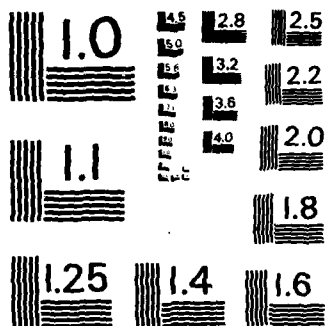|	1.0		2.8		2.5
	1.1		3.2		2.2
			3.6		2.0
			4.0		1.8
	1.25		1.4		1.6

MICROCOPY RESOLUTION TEST CHART
NATIONAL BUREAU OF STANDARDS-1963-A

REPORT DOCUMENTATION PAGE		READ INSTRUCTIONS BEFORE COMPLETING FORM
1. REPORT NUMBER INDU/DC/GMH/TR-84-61	2. GOVT ACCESSION NO.	3. RECIPIENT'S CATALOG NUMBER
4. TITLE (and Subtitle) A Detailed Consideration of Resonacne Radiation Trapping in the Argon Inductively Coupled Plasma		5. TYPE OF REPORT & PERIOD COVERED Interim Technical Report
		6. PERFORMING ORG. REPORT NUMBER 70
AUTHOR(s) J. W. Mills and G. M. Hieftje		8. CONTRACT OR GRANT NUMBER(s) N14-76-C-0838
PERFORMING ORGANIZATION NAME AND ADDRESS Department of Chemistry Indiana University Bloomington, IN 47405		10. PROGRAM ELEMENT, PROJECT, TASK AREA & WORK UNIT NUMBERS NR 051-622
CONTROLLING OFFICE NAME AND ADDRESS Office of Naval Research Washington, D.C.		12. REPORT DATE 9 March 1984
		13. NUMBER OF PAGES 21
4. MONITORING AGENCY NAME & ADDRESS(If different from Controlling Office)		15. SECURITY CLASS. (of this report) UNCLASSIFIED
		15a. DECLASSIFICATION/DOWNGRADING SCHEDULE

16. DISTRIBUTION STATEMENT (of this Report)

This document has been approved for public release and sale;
its distribution is unlimited.

17. DISTRIBUTION STATEMENT (of the abstract entered in Block 20, If different from Report)

18. SUPPLEMENTARY NOTES

Prepared for publication in SPECTROCHIMICA ACTA, PART B

19. KEY WORDS (Continue on reverse side If necessary and Identify by block number)

inductively coupled plasma
excitation mechanisms
elemental analysis
radiation trapping

20. ABSTRACT (Continue on reverse side If necessary and Identify by block number)

The extent and duration of trapping of argon resonance radiation (106.7 nm and 104.8 nm) in the ICP was calculated using a model incorporating line shape contributions from both Doppler and pressure broadening. The trap was found to be at the pressure-broadened limit, giving an escape factor of 7.9×10^{-4} when excitation of the 4s states in the plasma annulus is assumed. Theoretical apparent radiative lifetimes t_{app} for argon $^3P_1$ and $^1P_1$ resonance states are calculated to be 8 µs and 1.9 µs respectively. The quartet of 4s states, rapidly mixed by electron collisions, are presumed to share an overall .....cont.

AD A139369

DTIC FILE COPY

MAR 2 2 1984

84 03 22 055

20. Abstract (continued)

apparent radiative lifetime $\tau_{app} = 1.6$ µs for the purpose of plasma modeling. Effects of this radiation trapping on the argon 4s atom density and on electron-ion recombination are discussed.

OFFICE OF NAVAL RESEARCH

Contract N14-76-C-0838

Task No. NR 051-622

A DETAILED CONSIDERATION OF RESONANCE RADIATION TRAPPING

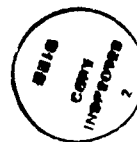IN THE ARGON INDUCTIVELY COUPLED PLASMA

by

J. W. MILLS AND G. M. HIEFTJE

INTRODUCTION

According to optical-depth calculations [1,2], 106.7 nm and 104.8 nm argon resonance radiation is extensively imprisoned within the argon inductively coupled plasma (ICP). This radiation trapping lengthens the apparent radiative lifetimes τ_{app} and would increase the populations of the radiative $^3P_1$ and $^1P_1$ argon 4s states if the main relaxation pathway were indeed radiative rather than collisional. Consequently, radiation trapping must be considered in developing both a plasma model and an analyte excitation mechanism for the ICP.

As argon 4s atoms decay radiatively, the resonance radiation is repeatedly self-absorbed and re-emitted within the argon stream. Radiative loss of the resonance energy occurs only as photons migrate to the stream boundaries. The degree of imprisonment can be described in terms of the probability that a given resonance photon will escape from the trap. This probability is commonly called the escape factor and is denoted g. The system behaves as if the radiative resonance states possess lengthened lifetimes. The resulting apparent radiative lifetime τ_{app} is longer than the natural radiative lifetime τ_o according to

$$\tau_{app} = \tau_o / g \; .\tag{1}$$

For the argon resonance lines in the ICP, g values of $10^{-5} - 10^{-6}$ have been calculated [1,2] using Holstein's theory for a cylindrical trap with Doppler-broadened line profiles [3,4]. This degree of imprisonment gives apparent lifetimes of approximately 1-10 ms for the argon $^3P_1$ and $^1P_1$ states. Experimental values for argon 4s lifetimes in the ICP, requiring spectroscopic measurements at 105 nm, have not yet been reported.

Radiation trapping is important in ICP modeling in several ways. Imprisoned resonance radiation maintains a suprathermal argon 4s population. (A rapid and complete collisional mixing of the quartet of 4s states is presumed [1,2,5].) In turn, the 4s population is of direct importance in assessing the contribution of Penning ionization to the analyte excitation picture. Furthermore, for plasmas in which the electron particle density n_e is near the threshold for local thermal equilibrium (LTE), resonance radiation trapping supports LTE by reducing the importance of radiative 4s decay relative to 4s relaxation by electron collisions [2,6-8]. Lastly, if apparent lifetimes are in the millisecond range [1], argon 4s atoms would permeate the argon plasma body and tailflame (to the extent that they are not collisionally deactivated).

Previous trapping calculations assumed the resonance absorption and emission line profiles both to be Gaussian because of Doppler broadening [1,2], in which case the escape factor depends inversely upon the ground state particle density n_o [3,4]. In contrast, for strongly self-absorbed lines, escape of radiation from a resonance trap would be caused largely by losses in the wings of the line profile [3,4]. Thus, trapping is particularly sensitive to the existence of pressure broadening and its Lorentzian-dominated contributions to the line profile wings. At n_o values where pressure broadening dominates the line wings, the escape factor g reaches a limiting value. For laboratory conditions this high-pressure limit is in the range $10^{-3} \leq g \leq 10^{-4}$.

The argon resonance lines in the ICP possess a significant pressure-broadening component, casting some doubt on earlier calculations [1,2]. The full width at half-maximum intensity (FWHM) for pressure broadening of the 104.8 nm line, for instance, is calculated for the ICP to be ~ 3×10^{-4} nm [9-11] compared with an estimated Doppler FWHM of 7×10^{-4} nm for a nominal

ICP gas temperature of 5000 $^\circ$K [10,12]. Although this calculated pressure-broadened component is seemingly less than that of the Doppler effect, its Lorentzian nature influences the line wings dramatically.

The Holstein model for a cylindrical radiation trap, employed previously for ICP modeling [1,2], presumes initial excitation of the resonance states along the axis of the cylinder [3,4]. In contrast, the actual excitation geometry of the ICP is annular, with 4s excitation occurring throughout the plasma region, presumably via the complex combination of electron (and atomic) collisions, ionization, recombination, and radiative cascading expected in a collision-dominated plasma [6].

These circumstances, and the lack of direct experimental lifetime measurements, encourage further development of resonance radiation trapping calculations for the argon ICP. In the present study, such calculations are provided and reveal that the radiation imprisonment is governed by pressure broadening. The resulting apparent lifetime τ_{app} is independent of the argon ground-state particle density n_0 and is considerably shorter than earlier calculations [1,2] indicated. The importance of resonance radiation trapping to the sustenance of the argon ICP is also considered in some detail.

THEORY

Theories of radiation transport through an optically thick medium have been developed for situations ranging from those in laboratory atomic spectroscopy to those in astrophysical plasmas [13]. Radiation imprisonment in the context of atomic radiative lifetime measurements has been modeled by Holstein [3,4] for pulsed excitation using a variational treatment, and numerically by Bieberman [14] for steady-state excitation conditions. The

two treatments are in essential agreement, with steady-state escape factors being 20 percent larger than the Holstein results for intermediate and large optical depths (greater than ~ 20). These trapping models have been extended by Walsh [15,16] and Phelps [17,18]. A number of experiments [17-25] have shown the agreement between experiment and theory to be generally better than 15 percent. Here we present a brief review of Holstein's theory [3,4] as it applies to the ICP, combining Doppler and pressure-broadening effects [16].

The transport of radiant energy through an optically thick medium can be described [3] by the rate of change of excited-state particle density n at location r according to

$$\frac{dn(r)}{dt} = \int_{\text{trap volume}} \gamma \, n(r') \, G(r,r') \, dr' - \gamma n(r) \qquad (2)$$

where γ is τ_o^{-1} and $G(r,r')dr'$ is the probability that radiation emitted at location r' is transmitted to r and captured (absorbed) there. The factor γ $n(r')$ gives the rate of emission from a volume element dr' at r'. The first term on the right-hand side of equation (2) thus describes the rate of formation of excited states at r by absorption of radiation emanating from all other locations in the trap. The second term simply describes the rate of excited-state loss at r by emission.

If one defines a transmission coefficient $T(\rho)$ to describe the probability that a photon emitted at r' travels the distance $\rho = |r-r'|$, the probability of photon capture over a distance $d\rho$ will be proportional to $-(\partial T/\partial \rho)d\rho$. For a photon emitted isotropically at r', the probability of that photon traveling within a solid angle $d\omega$ is $d\omega/4\pi$. The probability of photon capture $G(r,r')$ within a volume element $dr = \rho^2 d\rho d\omega$ located at r is

then

$$G(r,r') = -\frac{1}{4\pi\rho^2}\left(\frac{\partial T}{\partial \rho}\right) \tag{3}$$

Substituting equation (3) into equation (2) provides the rate expression to be solved. Non-radiative creation or annihilation of excited states can be included in this treatment by adding the appropriate terms [15,23].

Solving equation (2) is complicated by the fact that $T(\rho)$ depends upon the spectral distribution profile of emission and absorption. $T(\rho)$ can be written

$$T(\rho) = \int P(\nu) \exp[-k(\nu)\rho]\, d\nu \tag{4}$$

where the conventional transmission probability $\exp[-k(\nu)\rho]$ is averaged over the emission profile $P(\nu)$; $k(\nu)$ is the atomic absorption coefficient. For Doppler-broadening, $P(\nu)$ is proportional to $k(\nu)$ [13]. (Also see Appendix A of [4].)

Figure 1 illustrates the nature of $T(\rho)$. In Fig. 1 the absorption coefficient $k(\nu)$ has been given the Gaussian form $\exp[-(\nu-\nu_o)^2]$ and the optical depth $k\rho*$ has been assigned the value 6 at the line center, to describe a Doppler-broadened line whose center is strongly self-absorbed (Fig. 1c). For the sake of illustration, the emission profile $P(\nu)$ has been set equal to $k(\nu)$; for argon resonance lines in all regions of the ICP, $P(\nu)$ is calculated [16] to be $\ll k(\nu)$ and the magnitude of $T(\rho)$ is accordingly smaller than suggested in Fig. 1. From Fig. 1, the magnitude of $T(\rho)$ clearly derives from the wings of the line in a manner analogous to that

----

*The optical depth $k\rho$ is also known as absorbance or optical density.

found in the integrated intensity profile for a self-reversed atomic line.
In extreme cases, radiation trapping can spread resonance lines over many
tens of nanometers [26].

Equation (2) has for solutions a family of eigenfunctions of the form

$$n(r,t) = n(r) \exp[-g\gamma t] \qquad (5)$$

where g is the radiation trapping factor. Under pulsed excitation condi-
tions, the trap system would rapidly evolve to the $n(r,t)$ eigenfunction
having the smallest $g\gamma$ eigenvalue. This smallest $g\gamma$ value defines the
escape factor g, the apparent lifetime $\tau_{app} = (g\gamma)^{-1}$, and the corresponding
"standing wave" distribution $n(r)$. The evolution of this longest-lived
eigenfunction is complete within a period $t \ll (g\gamma)^{-1}$. For steady-state
excitation, this same longest-lived eigenfunction governs the predominate
standing-wave distribution, with contribution coefficients for higher eigen-
functions being inversely proportional to their corresponding eigenvalues.
Holstein has calculated $n(r)$ and g using the Ritz variational procedure [3],
with g taking the simple form

$$g \simeq g_o \, T(\rho) \qquad (6)$$

to within 3 percent. The constant g_o depends upon the choice of absorption
profile and trap geometry. In a cylindrical radiation trap, g_o is 1.9 for a
Doppler-broadened profile and 1.3 for one dominated by pressure broadening.
These values are based on Bieberman's steady-state solution [14], and are 20
percent larger than those of Holstein [3,4].

For a cylindrical radiation trap of radius R in which initial excitation is along the cylinder axis, the radial distribution of excited states n(r) is given by

$$n(r)/n(r=o) = [1 - \alpha r^2/R^2] \qquad (7)$$

where α is approximately 8/9 and 3/4 for the Doppler and pressure-broadened cases respectively. Figure 2 shows n(r) plotted versus r for these two cases. When the initial excitation is pulsed, the distribution is established within a period $t \ll (g\gamma)^{-1}$, i.e., $t \ll \tau_{app}$.

Walsh [16] has combined the effects of Doppler and pressure broadening under an approximate absorption coefficient $k(\nu)$:

$$k(\nu) = k_o[\exp(-x^2) + ax^2/\pi^{\frac{1}{2}}] \qquad (8)$$

where

$$x = (\nu - \nu_o) \lambda_o/v_o$$

$$a = (\gamma + \gamma_c) \lambda_o/4\pi v_o$$

$$k_o = \lambda_o^3 \, g_2\gamma n_o/8\pi^{3/2} \, g_1 v_o$$

$$\gamma_c = 4e^2 \, f\lambda_o n_o/3mc$$

v_o is the average particle velocity $(2RT/M)^{1/2}$, λ_o is the central wavelength of the transition, f is the oscillator strength, and g_2 and g_1 are the degeneracies of the excited and ground states respectively; γ_c is the average collision rate for the excited state, k_o is the absorption coef-

ficient at the line center, n_o is the number density of ground-state (absorbing) species, m is their mass, and e is the unit charge.

Using equations (4) and (8), $T(\rho)$ becomes

$$T(\rho) = T_D \exp(\pi T_{CD}^2/4T_C^2) + T_C E_2 \{\pi^{1/2} T_{CD}/2T_C\} \tag{9}$$

where

$$T_D = [k_o\rho(\pi \ln k_o\rho)^{1/2}]^{-1} \quad , \quad T_C = [a/\pi^{1/2}k_o\rho]^{1/2} \quad ,$$

and

$$T_{CD} = 2a/\pi(\ln k_o\rho)^{1/2} .$$

T_D and T_C are the transmission coefficients for pure Doppler and pressure broadening, respectively, and T_{CD} is the coefficient for pressure-broadened emission and Doppler-broadened absorption profiles. E_2 is the error integral [27] and is 1.0 for the argument values $^{1/2}T_{CD}/2T_C$ encountered in our calculation. Equation (9) reduces to T_C for large values of the damping coefficient $\underline{a}$ and to T_D as $\underline{a}$ vanishes, and agrees with experiment to within 10 percent [16]. The optical depth $k_o\rho$ pertains to the line center. For a cylindrical trap with axial excitation, ρ becomes the cylinder radius R.

RESULTS

Cylindrical trap-axial excitation. The transmission coefficient as a function of trap radius, $T(R)$, was calculated using equation (9) for a cylindrical trap of radius $R = 0.9$ cm containing argon at 1 atmosphere pressure and over a 300-10,000 °K range of gas temperature. Axial excitation was assumed. The temperature dependence of $T(R)$ derives simply from

the variation in particle velocity (v_o) and ground-state number density (n_o). Under these conditions, the optical depth $k_o R$ always exceeds 10^5. The transmission coefficient $T(R)$ was calculated to be 6.3×10^{-4} for all temperatures and for both argon resonance lines, despite their differing oscillator strengths (f is 0.07 and 0.28 for the 106.7 and 104.8 nm lines, respectively [9].) This calculated $T(R)$ value is the high-pressure limit T_c (cf. Eq. 9). For nominal ICP gas temperatures, the first (Doppler-dominated) term of equation (9) contributes significantly only as the number density n_o falls below 10^{17} cm^{-3}, which is a full order of magnitude below n_o in the atmospheric ICP.

Under these conditions and using equation (6), the escape factor g is calculated to be 8.2×10^{-4}, giving τ_{app} values of 10 µs and 2.4 µs for the $^3P_1$ and $^1P_1$ states, respectively. These values agree closely with direct lifetime measurements for pulsed electron-impact argon excitation at 300 °K [28]. The uncertainty in the trapping calculation is estimated to be 15 percent.

Cylindrical trap-ICP conditions. Unfortunately, the ICP differs from the foregoing Holstein-based cylindrical trap model, with its axial excitation, because of the annular argon 4s excitation in the ICP and the presence of electron-collision-induced 4s excitation and relaxation.

Walsh [15] addresses both of these factors for the case where electron-impact excitation permeates the trap, causing n(r) to be constant over the trap radius rather than following equation (7) (cf. Fig. 2). By Walsh's calculation, the escape factor is increased by 19% when an atom experiences many impact excitations and deactivations during the photon imprisonment period (τ_{app}). This model rests upon near thermal equilibrium between radiative and impact processes, with a steady state of excitation-deactiva-

tion. This situation pertains more closely to the ICP annular region than to the decaying plasma of the central channel and tailflame. In these latter regions, τ_{app} would be expected to decrease substantially as electron-impact deactivation leads to the loss of energy.

From Walsh's calculation, τ_{app} for the ICP annular region is probably best taken as 8.0 ($^3P_1$) and 1.9 μs ($^1P_1$).

There is ample evidence that the 4s states are equilibrated within a period near 10^{-9}s in a collision-dominated argon plasma such as the ICP [2,5]. It is then plausible to assume for plasma modeling that the 4s quartet shares a common apparent lifetime for the radiative loss of resonance energy. Because the $^3P_1$ and $^1P_1$ states have equal degeneracies, their radiative decay rates are simply additive ($\tau_{overall}^{-1} = \tau_1^{-1} + \tau_2^{-1}$). Thus the 4s apparent radiative lifetime effectively becomes 1.6 μs for the annular region, its enclosed central channel, and the tail flame, all of which share the cylindrical trap geometry with off-axis 4s excitation.

Effect of argon eximers on radiation trapping. The ICP is sufficiently dense in argon to consider the formation of Ar_2^* eximers from argon 4s atoms, with corresponding eximer emission at 126 nm and in the first continuum to the red of the 106.7 nm resonance line [28,30]. This eximer emission, which cannot be absorbed by ground-state argon atoms, would be lost from the radiation trap and would decrease the apparent lifetime τ_{app} accordingly [28]. Importantly, the ICP background spectrum shows no emission at 126 nm [31].

The rate of Ar_2^* formation in the ICP can be estimated, taking 1.6 x 10^{-32} cm^6 s^{-1} as the overall three-body rate constant for forming Ar_2^* from Ar ($^1P_1$, $^3P_1$, $^3P_2$) at 300 °K [32]. Adjusting the rate constant for a gas temperature of 5000 °K [33] and converting to an equivalent pseudo-first-order constant gives a value of 3 x 10^4 s^{-1} for an argon number density n_o =

1.5 x 10^{18} cm^{-3}. This rate is an order of magnitude slower than τ_{app}^{-1}.
However, as the gas temperature drops below about 2000 ^{O}K, the calculated
eximer formation rate surpasses τ_{app}^{-1}. Consequently, Ar$^{*}_{2}$ is most likely
present in the ICP argon coolant sheath and might affect radiation trapping
there, but probably does not appear to a significant degree in the central
plasma region or in the sample-containing area. Trap loss from eximer
emission is thus judged insufficient to shorten τ_{app} appreciably.

DISCUSSION

The degree to which resonance-radiation imprisonment maintains the
argon ICP depends primarily upon the electron number density n_e and on the
relative importance of electron-collisional and radiative processes. The
relative importance of these factors can be evaluated with the classic
Bates, Kingston and McWhirter (BKM) collisional-radiative model of a recom-
bining plasma [6]. This model is a detailed accounting of the various
collisional and radiative processes which contribute to the recombination of
electrons and ions in a dense plasma, with subsequent cascading of excited
states to the atomic ground state. The overall net rate of recombination,
or rate of decay of the plasma state, is expressed in terms of a simple two-
body ion-electron recombination process, incorporating the consequences of
the complex set of competing collisional and radiative excitation and re-
laxation events. The ICP would be expected to exhibit "recombining" behav-
ior [6] in the region downstream from the load coil, but not necessarily in
the central analyte-containing zone.

In the BKM model, net recombination is slowed by resonance radiation
trapping to the extent that the elevated resonance state population leads to
increased reionization. The effect of trapping is significant if n_e is

below a threshold value that depends weakly upon the electron temperature T_e. Above this threshold, n_e is sufficiently high that collisional processes dominate excitation and relaxation, and the radiative role is negligible. For argon plasmas at atmospheric pressure, the n_e threshold appears to be ~ 2×10^{16} cm^{-3}, based upon the condition for local thermodynamic equilibrium (LTE) in arc studies [2,34] in which T_e was 7000–9000 ^oK. Measurements of n_e in the ICP generally give values in the range 5×10^{14} to 1×10^{16} [35–37]. Consequently, one can assume that recombination in the ICP is retarded by resonance radiation trapping, with the effect being greatest at the plasma outer surface, in the sample stream, and in the tail flame, where n_e is lowest. BKM calculations for a hydrogen plasma [6] show that, as n_e drops a decade below the LTE threshold value at T_e ~ 4000 ^oK, resonance radiation trapping slows recombination by only 10 percent. Therefore, the retardation in recombination should not be dramatic except perhaps in the very uppermost region of the plasma tail flame.

The effect of resonance radiation imprisonment upon the argon 4s population is illustrated by the calculation of Giannaris and Incropera for an atmospheric argon arc plasma [7], also performed using the BKM recombination model. For $10^{15} \leq n_e \leq 10^{16}$ cm^{-3} and $7500 \leq T_e \leq 9500$ ^oK, complete resonance radiation trapping causes the 4s states to be overpopulated by 10 percent compared to the population predicted by the Saha equilibrium of Ar$^+$ with the assumed number of free electrons. Without trapping, the 4s states are calculated to be underpopulated by 50 percent, compared to the Saha value, as a consequence of radiational disequilibrium induced by the large 4s – 3p transition probability. For n_e the 2×10^{16} cm^{-3} LTE threshold described above, the BKM calculation gives Saha-based 4s populations, whether or not the resonance radiation is imprisoned.

In the ICP, the populations of the 4p (and higher) states should not be

significantly affected by resonance radiation trapping, except perhaps in regions of lowest n_e. Even in electron-lean regions of the ICP, the 4p and higher states would be expected to approach equilibrium with the 4s states. If, in these regions, the 4s population were elevated by radiation trapping, higher-energy states would be similarly affected.

For axial 4s excitation and in an Ar environment dominated by radiation trapping, the 4s radial population distribution $n_{4s}(r)$ would follow curve b of Fig. 2. However, from the BKM model [7], $n_{4s}(r)$ in the ICP should be determined primarily by electron collisions in regions of large n_e. Accordingly, in the annular skin region of the ICP, where n_e is high, $n_{4s}(r)$ should resemble the radial n_e distribution (with allowance for radial variations in electron energy distribution) and would likely be within 10 percent or so [7] of the LTE 4s population dictated by T_e and n_e. However, radiation imprisonment in regions of low n_e (e.g. in the aerosol channel) would have a significant impact. In these regions $n_{4s}(r)$ rises above that predicted by LTE.

In this regard, argon carrier gas in the central aerosol channel acts as a resonance radiation sink as it flows upward into the plasma core region. In the aerosol channel, n_{4s} should reach the steady-state value prescribed by radiation imprisonment within a period $t \ll \tau_{app}$ [3]. For $\tau_{app} = 1.6$ µs, we take this equilibrating period to be $< 10^{-7}$s. For a stream speed of 100 m/s near the sample-jet orifice [38], imprisonment equil   therefore established immediately as the carrier argon enters the pl.   . The radiative transfer which establishes this equilibrium and n_{4s} which results from it are independent of T_g.

Radiation trapping clearly predicts that, in the central channel, n_{4s} exceeds the value obtained from the central channel n_e and T_g under LTE.

The absolute magnitude of the central channel 4s population cannot be accurately determined from the trapping theory. However, it will certainly not exceed the highest annular value; an annular excitation temperature of 10000 - 12000 $^{\circ}$K gives $4 \times 10^{13} \leq n_{4s} \leq 4 \times 10^{14}$ cm^{-3} when the 4s quartet is considered a single level having 12-fold degeneracy and an energy of 11.7 eV. In an argon arc with an excitation temperature comparable to the ICP, Shindo and Imazu [39] found that, below $n_e \sim 2 \times 10^{16}$ cm^{-3}, n_{4s} is independent of n_e, largely because of radiation trapping. Their measurements indicate that the total 4s population density is approximately 1×10^{13} cm^{-3} in a non-LTE argon plasma with trapped resonance radiation. Uchida and coworkers [37] have recently reported relative radial $^3P_2$ distributions in the ICP which indicate that the central channel n_{4s} is substantially smaller than in the annular region, with the radial gradient diminishing with elevation and disappearing above an elevation of approximately 15 mm from the load coil.

CONCLUSIONS

Imprisonment of argon resonance radiation in the ICP is limited by losses caused by pressure broadening of the absorption-emission line profiles. The theoretical radiation escape factor g calculated for a cylindrical ICP radiation trap with annular argon 4s excitation (caused predominately by electron collisions), has a lower limit of 7.9×10^{-4}. Apparent radiative lifetimes τ_{app} are found to be 8 μs and 1.9 μs for the $^3P_1$ and $^1P_1$ argon resonance states, respectively. The quartet of 4s states, which are assumed to be completely interconverted by electron collisions under ICP conditions, share an overall apparent radiative lifetime τ_{app} of 1.6 μs. This apparent lifetime is independent of the argon gas temperature and relatively insensitive to whether the plasma state is dominated by radiative

or collision-induced processes.

Radiation trapping increases the argon 4s atom density n_{4s} by an estimated 10 percent over that predicted by LTE in the collision-dominated regions of the plasma wherever $n_e > 1 \times 10^{15}$ cm^{-3} (e.g. in the plasma "fireball"). Substantially larger deviations from LTE are predicted in regions (e.g. the central channel) where n_e falls well below this value. Radiation trapping is predicted to retard electron-ion recombination by 10 percent, which contributes to the ambient n_e and argon-ion concentrations. The trapping supports a suprathermal n_{4s} in the central aerosol channel at all elevations in the plasma.

From these considerations, radiation trapping would seem not to be responsible for sustaining the plasma well beyond the load-coil region, as earlier postulated by Blades and Hieftje [1]. The trapping lifetime of 1.6 µs reported here would support the discharge no more than 0.05 mm beyond the energy-addition zone, assuming a gas velocity of 30 m/s. Clearly, another mechanism for ICP maintenance must be sought; plasma modulation experiments, now underway in our laboratory, are directed at identifying the responsible process.

ACKNOWLEDGEMENT

REFERENCES

[1] M. W. Blades and G. M. Hieftje, Spectrochim. Acta 37B, 191 (1982).

[2] J. F. Alder, R. M. Bombelka, and G. F. Kirkbright, Spectrochim. Acta 35B, 163 (1980).

[3] T. Holstein, Phys. Rev. 72, 1212 (1947).

[4] T. Holstein, Phys. Rev. 83, 1159 (1951).

[5] S. Vacquie, J. P. Dinguirard, H. Kafrouni, and I. Pages, J. Quant. Spectrosc. Radiat. Transfer 17, 755 (1977).

[6] D. R. Bates, A. E. Kingston, and R. W. P. McWhirter, Proc. Roy. Soc. A270, 155 (1962); also D. R. Bates and A. Dalgarno in Atomic and Molecular Processes D. R. Bates, ed., pp. 253-7, Academic Press, New York (1962).

[7] R. J. Giannaris and F. P. Incropera, J. Quant. Spectrosc. Radiat. Transfer 13, 167 (1973).

[8] H. R. Griem, Plasma Spectroscopy p. 151, McGraw-Hill, New York (1964).

[9] G. H. Copley and D. M. Cann, J. Quant. Spectrosc. Radiat. Transfer 14, 899 (1974).

[10] D. N. Stacey and J. M. Vaughan, Phys. Lett. 11, 105 (1964).

[11] D. P. Aeschliman, R. A. Hill, and D. L. Evans, Phys. Rev. A 14, 1421 (1976).

[12] G. Bekefi, C. Deutsch, and B. Yaakobi, Principles of Laser Plasmas G. Bekefi, ed., pp. 576-7. J. Wiley, New York (1976).

[13] D. G. Hummer, J. Quant. Spectrosc. Radiat. Transfer 8, 193 (1968).

[14] L. M. Bieberman, J. Exptl. Theoret. Phys (JETP) USSR 17, 416 (1947); 19, 584 (1949).

[15] P. J. Walsh, Phys. Rev. 107, 338 (1957).

[16] P. J. Walsh, Phys. Rev. 116, 511 (1959).

[17] A. V. Phelps, Phys. Rev. 110, 1362 (1958).

[18] A. V. Phelps, Phys. Rev. 114, 1011 (1959).

[19] L. M. Bieberman and I. M. Gourevitch, J. Exptl. Theoret. Phys. (JETP) USSR 19, 507 (1949); 20, 108 (1950).

[20] D. Alpert, A. O. McCoubrey, and T. Holstein, Phys. Rev. 76, 1259 (1949).

[21] T. Holstein, D. Alpert, and A. O. McCoubrey, Phys. Rev. 85, 985 (1952).

[22] R. G. Bennett and F. W. Dalby, J. Chem. Phys. 31, 434 (1959).

[23] A. V. Phelps, Phys. Rev. 117, 619 (1960).

[24] A. V. Phelps and A. O. McCoubrey, Phys. Rev. 118, 1561 (1960).

[25] J. Z. Klose, Phys. Rev. 188, 45 (1969).

[26] B. E. Douda and E. J. Bair, J. Quant. Spectrosc. Radiat. Transfer 14, 1091 (1974).

[27] E. Jahnke and F. Emde, Tables of Higher Functions, 5th Edition, p. 24. B. G. Teubner Verlagsgesellschaft, Leipzig (1952).

[28] N. Thonnard and G. S. Hurst, Phys. Rev. A 5, 1110 (1972).

[29] S. Heron, R. W. P. McWhirter, and E. H. Rhoderick, Proc. Roy. Soc. (London) A234, 565 (1956).

[30] M. H. R. Hutchinson, Appl. Phys. 21, 95 (1980).

[31] D. R. Heine, J. S. Babis, and M. B. Denton, Appl. Spectrosc. 34, 595 (1980).

[32] M. Bourene, O. Dutuit, and J. Le Calve, J. Chem. Phys. 63, 1668 (1975).

[33] F. E. Niles and W. W. Robertson, J. Chem. Phys. 42, 3277 (1965).

[34] J. Bacri, A. M. Gomes, and S. Benzaid, _J. Phys. D. Appl. Phys._ **9**, 1743 (1976).

[35] D. J. Kalnicky, V. A. Fassel, and F. N. Kniseley, _Appl. Spectrosc._ **31**, 137 (1977).

[36] G. R. Kornblum and L. de Galan, _Spectrochim. Acta_ **32B**, 71 (1977).

[37] H. Uchida, K. Tanabe, Y. Nojiri, H. Haraguchi, and K. Fuwa, _Spectro-chim. Acta_ **36B**, 711 (1981).

[38] R. M. Barnes and R. G. Schleicher, _Spectrochim. Acta_ **36B**, 81 (1981).

[39] H. Shido and S. Imazu, _J. Quant. Spectrosc. Radiat. Transfer_ **23**, 605 (1980).

FIGURE CAPTIONS

Figure 1. Illustration of the nature of the transmission coefficient $T(\rho)$

for a strongly self-absorbed Gaussian line: a. Gaussian profile

for absorption coefficient $k(\nu)$ and emission profile $P(\nu)$. b.

Transmittance $\exp[-k(\nu)\rho]$. c. $P(\nu) \exp[-k(\nu)\rho]$. $T(\rho)$ is the

area under curve c according to equation (4). For b, k is taken

as 6 at the line center to give strong self-absorption. Note

that for argon resonance radiation in the ICP, $P(\nu) \ll k(\nu)$,

and $T(\rho)$ is appropriately smaller than portrayed here.

Figure 2. Calculated steady-state radial distribution of excited states

$n(r)$ in a cylindrical radiation trap of radius R with initial

excitation along the cylinder axis a. Doppler line profile. b.

Pressure-broadened profile. Both distribution curves have been

normalized to the same peak value.

n(ex)

radial position r/R

a

b
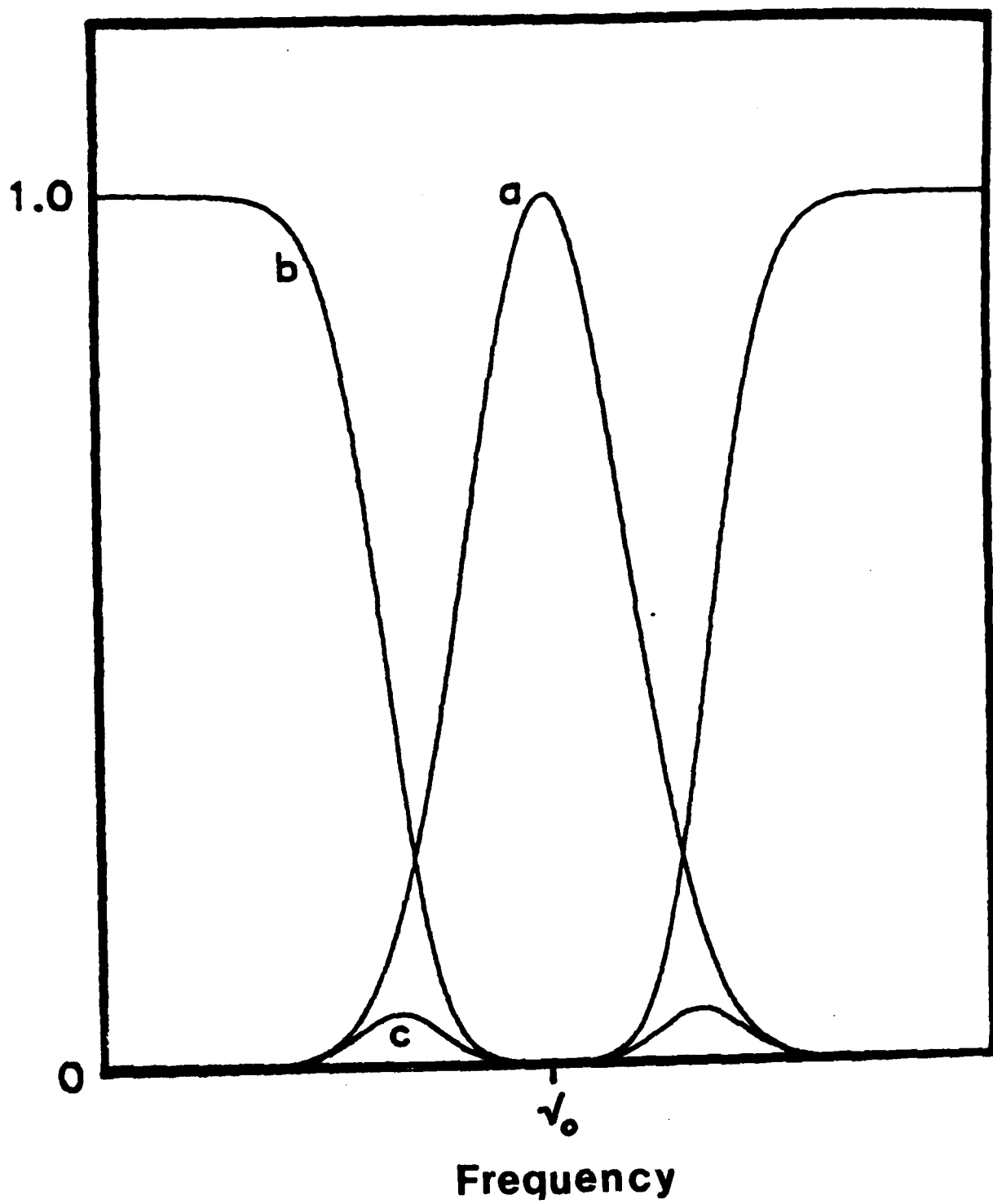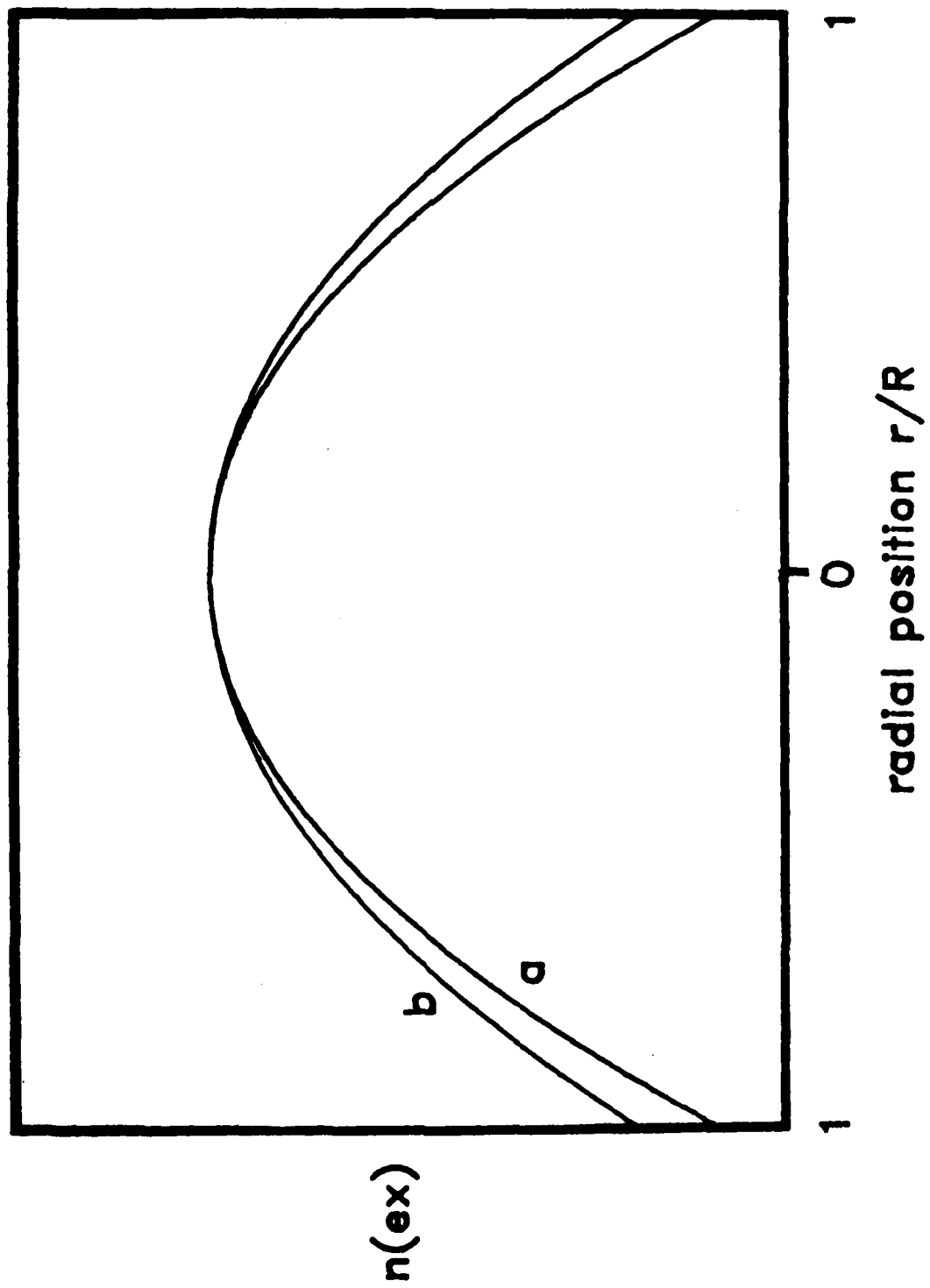
TECHNICAL REPORT DISTRIBUTION LIST, 051B

Professor J. Janata
Department of Bioengineering
University of Utah
Salt Lake City, Utah 84112

Dr. Denton Elliott
AFOSR/NC
Bolling AFB
Washington, D.C. 20362

Dr. J. DeCorpo
NAVSEA
Code 05R14
Washington, D.C. 20362

Dr. B. E. Spielvogel
Inorganic and Analytical Branch
P.O. Box 12211
Research Triangle Park, NC 27709

Dr. Charles Anderson
Analytical Chemistry Division
Athens Environmental Laboratory
College Station Road
Athens, Georgia 30613

Ms. Ann De Witt
Material Science Department
160 Fieldcrest Avenue
Raritan Center
Edison, New Jersey 08818

Dr. Ron Flemming
B 108 Reactor
National Bureau of Standards
Washington, D.C. 20234

Dr. A. Harvey
Code 6110
Naval Research Laboratory
Washington, D.C. 20375

Dr. David M. Hercules
Department of Chemistry
University of Pittsburgh
Pittsburgh, Pennsylvania

Dr. John Hoffsommer
Naval Surface Weapons Center
Building 30 Room 208
Silver Spring, Maryland 20910

Dr. Frank Herr
Office of Naval Research
Code 422CB
800 N. Quincy Street
Arlington, Virginia 22217

Mr. S. M. Hurley
Naval Facilities Engineering Command
Code 032P
200 Stovall Street
Alexandria, Virginia 22331

Professor E. Keating
Department of Mechanical Engineering
U.S. Naval Academy
Annapolis, Maryland 21401

Ms. W. Parkhurst
Naval Surface Weapons Center
Code R33
Silver Spring, Maryland 20910

Dr. M. H. Miller
1133 Hampton Road
Route 4
U.S. Naval Academy
Annapolis, Maryland 21401

Dr. M. Robertson
Electrochemical Power Sources Division
Code 305
Naval Weapons Support Center
Crane, Indiana 47522

Dr. Clifford Spiegelman
National Bureau of Standards
Room A337 Bldg. 101
Washington, D.C. 20234

CDR Andrew T. Zander
10 Country Club Lane
ONR Boston
Plaistow, New Hampshire 03865

TECHNICAL REPORT DISTRIBUTION LIST, 051B

Dr. Robert W. Shaw
U.S. Army Research Office
Box 12211
Research Triangle Park, NC 27709

Dr. Marvin Wilkerson
Naval Weapons Support Center
Code 30511
Crane, Indiana 47522

Dr. J. Wyatt
Naval Research Laboratory
Code 6110
Washington, D.C. 20375

Dean William Tolles
Naval Post Graduate School
Spanaugel Hall
Monterey, California 93940

Dr. H. Wohltjen
Naval Research Laboratory
Code 6170
Washington, D.C. 20375

TECHNICAL REPORT DISTRIBUTION LIST, GEN

	No. Copies		No. Copies
Office of Naval Research Attn: Code 413 800 N. Quincy Street Arlington, Virginia 22217	2	Naval Ocean Systems Center Attn: Technical Library San Diego, California 92152	1
ONR Pasadena Detachment Attn: Dr. R. J. Marcus 1030 East Green Street Pasadena, California 91106	1	Naval Weapons Center Attn: Dr. A. B. Amster Chemistry Division China Lake, California 93555	1
Commander, Naval Air Systems Command Attn: Code 310C (H. Rosenwasser) Washington, D.C. 20360	1	Scientific Advisor Commandant of the Marine Corps Code RD-1 Washington, D.C. 20380	1
Naval Civil Engineering Laboratory Attn: Dr. R. W. Drisko Port Hueneme, California 93401	1	Dean William Tolles Naval Postgraduate School Monterey, California 93940	1
Superintendent Chemistry Division, Code 6100 Naval Research Laboratory Washington, D.C. 20375	1	U.S. Army Research Office Attn: CRD-AA-IP P.O. Box 12211 Research Triangle Park, NC 27709	1
Defense Technical Information Center Building 5, Cameron Station Alexandria, Virginia 22314	12	Mr. Vincent Schaper DTNSRDC Code 2830 Annapolis, Maryland 21402	1
DTNSRDC Attn: Dr. G. Bosmajian Applied Chemistry Division Annapolis, Maryland 21401	1	Mr. John Boyle Materials Branch Naval Ship Engineering Center Philadelphia, Pennsylvania 19112	1
Naval Ocean Systems Center Attn: Dr. S. Yamamoto Marine Sciences Division San Diego, California 91232	1	Mr. A. M. Anzalone Administrative Librarian PLASTEC/ARRADCOM Bldg 3401 Dover, New Jersey 07801	1

TECHNICAL REPORT DISTRIBUTION LIST, 051B

Dr. M. B. Denton
Department of Chemistry
University of Arizona
Tucson, Arizona 85721

Dr. R. A. Osteryoung
Department of Chemistry
State University of New York
Buffalo, New York 14214

Dr. J. Osteryoung
Department of Chemistry
State University of New York
Buffalo, New York 14214

Dr. B. R. Kowalski
Department of Chemistry
University of Washington
Seattle, Washington 98105

Dr. H. Freiser
Department of Chemistry
University of Arizona
Tucson, Arizona 85721

Dr. H. Chernoff
Department of Mathematics
Massachusetts Institute of Technology
Cambridge, Massachusetts 02139

Dr. A. Zirino
Naval Undersea Center
San Diego, California 92132

Professor George H. Morrison
Department of Chemistry
Cornell University
Ithaca, New York 14853

Dr. Alan Bewick
Department of Chemistry
Southampton University
Southampton, Hampshire
ENGLAND 5095NA

Dr. S. P. Perone
Lawrence Livermore Laboratory L-370
P.O. Box 808
Livermore, California 94550

Dr. L. Jarvis
Code 6100
Naval Research Laboratory
Washington, D.C. 20375

Dr. G. M. Hieftje
Department of Chemistry
Indiana University
Bloomington, Indiana 47401

Dr. Christie G. Enke
Department of Chemistry
Michigan State University
East Lansing, Michigan 48824

Dr. D. L. Venezky
Naval Research Laboratory
Code 6130
Washington, D.C. 20375

Walter G. Cox, Code 3632
Naval Underwater Systems Center
Building 148
Newport, Rhode Island 02840

Professor Isiah M. Warner
Department of Chemistry
Emory University
Atlanta, Georgia 30322

Dr. Kent Eisentraut
Air Force Materials Laboratory
Wright-Patterson AFB, Ohio 45433

Dr. Adolph B. Amster
Chemistry Division
Naval Weapons Center
China Lake, California 93555

Dr. B. E. Douda
Chemical Sciences Branch
Code 50 C
Naval Weapons Support Center
Crane, Indiana 47322

Dr. John Eyler
Department of Chemistry
University of Florida
Gainesville, Florida 32611

END

FILMED

4-84

DTIC